High-Pressure Raman Noncoincidence Effect and Conformation of Alkyl Side Chain in Alkyl Benzoates

Vivian L. Slager, Hai-Chou Chang, Yoo Joong Kim, and Jiri Jonas*

Department of Chemistry, School of Chemical Sciences, and Beckman Institute for Advanced Science and Technology, University of Illinois, Urbana−Champaign, 166 Roger Adams Laboratory, 600 S. Matthews, Urbana, Illinois 61801

Received: June 10, 1997; In Final Form: September 17, 1997[⊗]

The Raman noncoincidence effect has been used to investigate the changes in intermolecular interactions induced by applying high pressure to neat liquid alkyl benzoates. The noncoincidence of the carbonyl band of a homologous series of straight chain alkyl benzoates (methyl, ethyl, propyl, butyl, and hexyl benzoate) and a branched chain alkyl benzoate (2-ethylhexyl benzoate) was measured at 20 and 40 °C over the pressure range 1−5000 bar. The density was measured as a function of pressure for all molecules. A transition point dividing the noncoincidence behavior as a function of density into two regions was found, for all molecules except methyl benzoate. Below the transition point, at lower density, the noncoincidence value was relatively insensitive to changes in density, while above the transition point, the noncoincidence value dropped sharply with increasing density. The decrease in the value of noncoincidence above the transition point was interpreted as the change in intermolecular interactions resulting from the conformational change in favor of a "folded" form of the alkyl side chain shielding the carbonyl group. To examine the plausibility of the presence of energetically allowable conformations with a folded alkyl side chain, conformational searches based on molecular mechanics calculations have also been performed. The strain energy of some alkyl benzoate conformers with folded side chain was calculated to be within a few kcal/mol of the global minimum conformation. Both the experimental results and the conformational analysis suggest that the population of the folded conformer increases under high-pressure conditions owing to its compactness.

Introduction

Arising from the coupling of a vibrational mode with the same vibration in neighboring molecules, the Raman noncoincidence effect has been used as a measure of intermolecular interaction. Commonly associated with the Raman bands that are also strongly IR active, this effect has been observed in various vibrational modes, most frequently in the C═O stretching modes of carbonyl compounds, such as acetone,[1−3] formamide,[4] *N*,*N*-dimethylformamide,[5,6] *N*,*N*-dimethylacetamide,[4] cyclic carbonates,[7,8] cyclohexane,[9] and methyl ethyl ketone.[10] The interaction between the vibrational modes of two different molecules leads to a frequency difference between the anisotropic and isotropic Raman bands. The noncoincidence effect is defined as

$$\Delta\nu = \nu_{\text{aniso}} - \nu_{\text{iso}} \tag{1}$$

Several theories have been developed to explain the noncoincidence effect, notably by Wang and McHale,[11−13] Fini and Mirone,[14,15] and Logan.[16−18] Since the C═O stretching modes have large transition dipole moments, the noncoincidence effect in these bands is considered to arise from the resonant transfer of vibrational excitation via transition dipole−transition dipole coupling.[10,17,18] The interactions between the transition dipoles of neighboring molecules have a different effect on the isotropic and anisotropic components of the Raman scattering tensor when there is local order present in the system. The isotropic part of the Raman spectrum reflects the spherically symmetric average of the intermolecular and intramolecular forces and is independent of orientation, whereas the anisotropic part reflects the effects due to angular dependence of interactions.[10−12,18] This leads to differences in the peak frequency as well as in the band shapes between the anisotropic and isotropic spectra. The magnitude of the noncoincidence splitting is generally considered to reflect the degree of interaction between two molecules or, more specifically, two vibrating dipoles.

Several studies have been performed employing temperature and/or pressure as experimental variables in order to investigate the sources contributing to the noncoincidence effect and their dependence on temperature and pressure. The temperature dependence of the noncoincidence effect is equivocal. For some systems, the $\Delta\nu$ values decrease with increasing temperature.[7,19] This has been interpreted to be due to the partial breakdown of regular short-range order of the liquid structure or faster reorientation of the molecules at higher temperature averaging out the interactions that are responsible for the noncoincidence effect. The opposite trend has been observed for the molecules where a resonance structure[4] or hydrogen-bonding structure[20,21] is present, which may be due to the effect of temperature on these structures. Regarding the effect of pressure,[2,4,7,20,21] the noncoincidence generally increases with an increase in density, as the molecular distances between neighboring molecules become smaller, increasing the intermolecular interaction which increases the coupling of the two transition dipoles.

2-Ethylhexyl benzoate (EHB) has been studied extensively using NMR,[22−26] infrared,[27,28] and Raman[29] spectroscopies as a model compound for elastohydrodynamic lubrication. A previous experiment in our laboratory[26] using 2D NOESY found cross peaks appearing at the elevated pressure, indicating possible space dipolar coupling between the aromatic protons and the methyl protons on the ends of the alkyl chains in EHB. Furthermore, the intensity of the cross peaks increased with pressure. These experimental results were explained by the approach of a methyl group to the ring at higher density by the bending of alkyl chain toward the aromatic ring. Simple force

* Corresponding author. Phone (217) 333-2572; Fax (217) 244-3993.
[⊗] Abstract published in *Advance ACS Abstracts,* November 1, 1997.

S1089-5647(97)01896-8 CCC: $14.00

field calculations suggest that the energy penalty for bending the alkyl chain toward the ring is small.[26]

When the alkyl chain of EHB is "folded" toward the benzene ring, it is expected to somewhat shield the carbonyl group of the benzoate from the carbonyl in a neighboring molecules. Since the noncoincidence effect reflects the interaction between two vibrational modes, the noncoincidence measurements for the C═O bands allow one to estimate the degree of shielding of the carbonyl group by the folding of the alkyl side chain. In the present study, we have measured the noncoincidence effect for a homologous series of alkyl benzoates: methyl benzoate (MB), ethyl benzoate (EB), propyl benzoate (PB), butyl benzoate (BB), and hexyl benzoate (HB), as well as EHB. By examining the noncoincidence effect of benzoates of various alkyl chains as a function of pressure, we hope to obtain the information about the conformational preferences of the alkyl chain in these complex liquids. In addition, by varying the length of the alkyl chain of the benzoate, the effect of chain length on the conformational change can be investigated.

In this study, density is an important experimental variable. Using the Tait equation and a high-pressure density meter, high-pressure Raman experiments can be done at known density. High-pressure Raman experiments have been performed in our laboratory on many systems, examining effects such as collision-induced scattering,[30,31] vibrational dephasing,[32,33] reorientational correlation,[34,35] and noncoincidence.[1,4,7,8,20,21] These experiments showed the importance of pressure as an experimental variable for the separation of the effects of internal energy and density and for modifying the intermolecular potential and relaxation processes. One of the important molecular level changes in liquids induced by external pressure is conformational changes in the molecules.[36,37] In fact, pressure is effective in perturbing the distribution of the conformers of hydrocarbon chain molecules.[38,39] Under the condition of high pressure, the conformational preferences are determined principally by the relative volume of the conformers, which is likely to be sensitive to the conformational changes due to folding of alkyl chain. Despite the relevance to understanding many important questions in functional fluids,[27] polymers,[40] and biomembrane lipids,[41,42] the pressure-induced conformational changes of hydrocarbon chains[38,39,43,44] have not been extensively studied. This is mostly due to the insensitivity[27,43] or questionable correspondence[44,45] of the conventional experimental parameters to the populations of trans/gauche conformations.

It should be noted that the individual conformers, especially with different conformations of the flexible alkyl chain, as in the present case, cannot be isolated or detected at normal experimental conditions. One can only observe the physical properties averaged over all the existing conformers in proportion to their relative populations. Due to the lack of a theory that can relate the noncoincidence value with geometric parameters of interacting molecules and also with the large amount of possible conformations available for the flexible ester side chains, the quantitative analysis of experimental data in terms of individual conformers is out of the question. As an alternative, a conformational search based on molecular mechanics calculations has been performed for the alkyl benzoates. This investigation is meaningful since by separately examining the individual conformers one can estimate the effect of thermodynamic variables on the conformational changes and possible interactions of the molecules from the consideration of the relative energy and the molecular shape of each conformer.

The general procedure of conformational search can be summarized[46,47] as (i) generating a crude starting geometry, (ii) optimizing its structure using molecular mechanics energy minimization algorithm, (iii) comparing the resultant energy-minimized conformer with previously found conformers to avoid duplication, and (iv) repeating the cycle by obtaining a new starting geometry. Since the energy minimization part of the process simply refines starting geometry to nearby local minimum on potential energy surface, the starting geometry generation step directly controls the overall effectiveness and thoroughness of the conformational search. Depending on the size (the number of rotatable bonds) and the type (boundary conditions to be applied) of the molecules, the methods employed to generate the starting geometries vary widely[47−49] from deterministic (grid) searches, which cover all areas on conformational surface systematically by varying each torsional angle in steps of predetermined degree, to stochastic methods, which use a random element for exploring the conformational space. Usually the conformational search is performed to find all of the stable local minima in the conformational space within a threshold value, say, 3−4 kcal/mol of the global minimum (lowest energy conformation), if possible. Practically, the relative population of a conformer is determined by the depth (energy) as well as the width (statistical weight or entropy) of the potential well of the local minimum corresponding to the conformer. Being unable to contribute the population appreciably, the high-energy conformers beyond the threshold value are generally ignored in the conformational search.

The objective of the conformational search is to identify all the low-energy conformations of the various alkyl benzoates and examine the plausibility of folded conformation of the alkyl chains. Despite the qualitative results of the conformational search, it supports our explanation for the pressure-dependent change of the Raman noncoincidence values in the alkyl benzoate system.

The main goal of this study is to determine the conformational changes of the alkyl side chain, which affect the intermolecular interactions measured by the Raman noncoincidence effect, in a series of homologous alkyl benzoates as a function of thermodynamic state. The noncoincidence of EHB will also be determined and compared to the straight chain homologous series to examine the effect of chain branching. Conformational analysis is used to corroborate the experimental results that suggest a folded alkyl chain conformation at high pressures.

Experimental Section

Materials. MB (99%), EB (99%), PB (99%), and BB (99%) samples were purchased from Aldrich Chemical Co., and HB (98+%) was from TCI. EHB (≥99.5%) was synthesized by Palmer Research Ltd. (U.K.). All the compounds except EB were used without further purification. The commercial EB sample contained a fluorescent contaminant, which was removed by distillation before use.

High-Pressure Density Measurements. The $P-V-T$ conditions used in this experiment were obtained using a home-built high-pressure relative density meter[50] and a commercial absolute density meter (Anton/Paar DMA 45 digital density meter). The high-pressure density was measured at 20 and 40 °C over the pressure range 1−5000 bar. Calibration of the instrument for each isotherm was achieved by using the densities measured at 1 bar at each temperature with the absolute density meter. MB and BB at 20 °C showed a phase transition at about 2000 bar, beyond which the density could not be measured. The experimental densities as a function of pressure for each temperature were fit to the Tait equation[30,51]

$$\rho_R(1/\rho_R - 1/\rho_P) = C \ln[(B + P)/(B + P_R)] \qquad (2)$$

where ρ_R is the density at the reference pressure P_R (1 bar), ρ_P

TABLE 1: Results of the Tait Equation Fitting of the Density Measurements for the Alkyl Benzoates (*B* in bar, ρ in g cm^{-3})

	20 °C			40 °C		
	ρ	*B*	*C*	ρ	*B*	*C*
methyl benzoate	1.0887	1540	0.088 82	1.0677	1515	0.094 85
ethyl benzoate	1.0481	1529	0.092 63	1.0188	1457	0.092 52
propyl benzoate	1.0230	1329	0.086 63	1.0057	1267	0.087 22
butyl benzoate	1.0050	1524	0.095 28	0.9871	1273	0.087 57
hexyl benzoate	0.9810	1911	0.105 00	0.9650	1278	0.087 02
2-ethylhexyl benzoate	0.9650	1443	0.098 26	0.9495	1261	0.085 51

is the density at the pressure *P*, and *B* and *C* are the Tait parameters for each isotherm. The fitted Tait parameter values and the densities at 1 bar are given in Table 1. The accuracy of the density measurements is estimated at ±5%.

High-Pressure Raman Experiments. Details of the high-pressure Raman cell and the high-pressure setups have been described previously.[52] The Raman excitation source was 488 nm radiation from an argon ion laser, which was used at a power of 0.6 W for all spectra. A double monochromator (Spex 1403) and a liquid nitrogen-cooled CCD detector operated at −110 °C (Princeton Instruments) were used to collect the scattered light. The CCD detector system consists of a thinned, back-illuminated 1024 × 1024 pixel chip manufactured by Tektronics. A neon lamp was used for calibration. An ethylene glycol and water bath (MGW Lauda Brinkmann RM6) was used to control the temperature. Raman spectra for the carbonyl band of each sample were collected over the range 1610−1830 cm^{-1}. The laser light was polarized vertically, and the scattered light was collected with both vertical (I_{VV}) and horizontal (I_{VH}) polarizations. Eight measurements were made for each sample at both 20 and 40 °C, except for PB at 20 °C for which 16 measurements were made. The average error in locating the peak frequencies calculated from the standard deviation was 0.3 cm^{-1}.

Molecular Mechanics Calculations. Conformational searches and molecular mechanics energy minimizations were performed using Universal Force Field (UFF)[53,54] as implemented in the program Cerius2 (BIOSYM/Molecular Simulations) on Silicon Graphics Indigo or O2 workstations. The minimization procedures were performed by the conjugate gradient method[55] until the root-mean-square value of the potential gradient was below 0.01 kcal mol^{-1} Å^{-1}. The UFF is a generic force field, and a test of its applicability to various organic molecules[54] showed that it correctly reproduced molecular structures and conformational energies. The errors in UFF predicted bond lengths and bond angles are slightly larger than those seen for the most popular MM2/MM3 force fields specialized for organic molecules. We believe that the UFF parameters are sufficiently accurate for the conformational search for alkyl benzoates because only a qualitative insight to the possible conformers of the alkyl benzoates is needed.

Results

Raman Noncoincidence Effect. Isotropic and anisotropic parts of spectrum are calculated from I_{VV} and I_{VH}, respectively, by using the equations

$$I_{aniso}(\nu) = {}^4/_3 I_{VH}(\nu)$$

$$I_{iso}(\nu) = I_{VV}(\nu) - {}^4/_3 I_{VH}(\nu) \quad (3)$$

From these spectra the noncoincidence value, $\Delta\nu$, is calculated according to eq 1. Figure 1 shows a typical pair of anisotropic and isotropic spectra for the C═O stretching band. The carbonyl bands for all of the neat benzoate samples were asymmetric. This phenomenon, probably due to hot bands interfering with the fundamental C═O band, has been observed in other carbonyl compounds,[1,2,4,5] and the asymmetry is on the high wavenumber side of the peak. To determine the correct band center, the undisturbed low wavenumber side of the peak was fitted using the method discussed extensively in our earlier study of carbonyl compounds.[2,7]

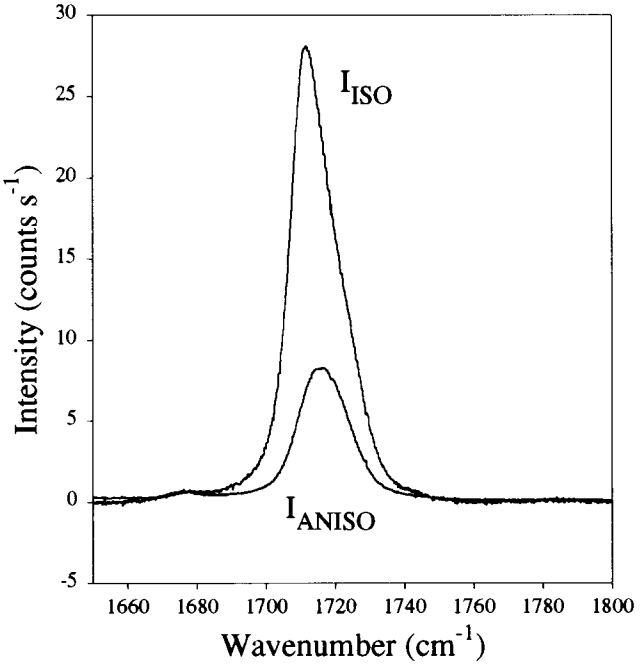

Figure 1. Anisotropic (I_{aniso}) and isotropic (I_{iso}) spectra of the carbonyl band of propyl benzoate at 20 °C and 2459 bar.

For all of the benzoates, $\Delta\nu$ values measured at the same density at two different temperatures (20 and 40 °C) were not different within experimental error, and no noticeable effect of temperature was found. Therefore, we averaged the data measured at 20 and 40 °C together for further analysis. For MB and BB, the data points above 2 kbar are measured only at 40 °C, because MB and BB become solid above 2000 bar at 20 °C. The average value of $\Delta\nu$ for each compound as a function of density (ρ) is shown in Table 2. $\Delta\nu$ measured at 20 and 40 °C for MB and BB are reported separately.

The noncoincidence of the alkyl benzoates as a function of molar volume ($V_M = M/\rho$; *M* is molecular weight) is shown in Figure 2. As shown in the figure, the behavior of $\Delta\nu$ for the carbonyl band of the various alkyl benzoates when reducing molar volume by external pressure can be divided into two regions. At high molar volume, the lower pressure region, the noncoincidence value was relatively insensitive to decreasing molar volume. A transition in the effect of decreasing molar volume was observed, and below that point the noncoincidence decreased sharply with decreasing molar volume. This kind of transition was not observed in MB, in which $\Delta\nu$ is insensitive to changes in molar volume throughout the whole pressure range investigated. To compare directly the noncoincidence behavior for various alkyl benzoates, $\Delta\nu$ is plotted as a function of packing fraction (ρ^*) in Figure 3. The packing fraction is defined by

$$\rho^* = V_W/V_M \quad (4)$$

where V_W is the (molar) van der Waals volume or the net volume occupied by the molecules excluding free volume. V_W was calculated by Bondi's method[56] of additive molecular group

TABLE 2: Average Noncoincidence Values for the Alkyl Benzoates; EB, PB, HB, and EHB Are the Average of 20 and 40 °C

	ρ (g cm^{-3})	V_M (cm^3)	packing fraction	$\Delta\nu$ (cm^{-1})
methyl benzoate (20 °C)	1.101	123.7	0.604	4.5
	1.126	120.9	0.618	4.5
	1.151	118.3	0.631	4.4
methyl benzoate (40 °C)	1.075	126.7	0.590	4.4
	1.100	123.8	0.604	4.3
	1.125	121.0	0.617	4.4
	1.150	118.4	0.631	4.5
	1.175	115.9	0.645	4.5
	1.200	113.5	0.659	4.5
ethyl benzoate	1.050	143.0	0.594	3.6
	1.075	139.7	0.608	3.6
	1.100	136.5	0.622	3.5
	1.125	133.5	0.636	3.5
	1.150	130.6	0.650	3.4
	1.175	127.8	0.665	3.2
	1.200	125.2	0.679	3.1
propyl benzoate	1.025	160.2	0.594	4.1
	1.050	156.4	0.609	4.1
	1.075	152.7	0.623	4.1
	1.100	149.3	0.638	4.0
	1.125	146.0	0.652	3.8
	1.150	142.7	0.667	3.4
	1.175	139.7	0.681	3.2
butyl benzoate (20 °C)	1.028	173.4	0.608	4.2
	1.055	168.9	0.624	4.2
	1.081	164.9	0.639	4.1
	1.107	161.0	0.655	3.9
butyl benzoate (40 °C)	1.000	178.2	0.591	4.0
	1.025	173.9	0.606	4.1
	1.050	169.7	0.621	4.2
	1.075	165.8	0.636	4.1
	1.100	162.0	0.651	3.8
	1.125	158.4	0.665	3.2
hexyl benzoate	1.000	206.3	0.610	3.8
	1.025	201.2	0.625	3.9
	1.050	196.5	0.641	3.8
	1.075	191.9	0.656	3.6
	1.100	187.5	0.671	3.3
	1.125	183.4	0.686	2.8
2-ethylhexyl benzoate	0.950	245.6	0.597	3.4
	0.975	239.3	0.612	3.5
	1.000	233.3	0.628	3.6
	1.025	227.6	0.644	3.5
	1.050	222.2	0.660	3.6
	1.075	217.0	0.675	3.5
	1.100	212.1	0.691	3.0
	1.125	207.4	0.707	2.5

volume increments. The packing fraction (ρ^*) as well as the molar volume (V_M) is included in Table 2. In Figure 3, the lines are drawn to show clearly the two regions of the effect of changes in packing fraction. Here the trends mentioned above are very obvious, and the transition points are clearly seen where two lines representing each regime showing the different pressure-dependent $\Delta\nu$ behavior cross. Moreover, the location of the transition point between the two regimes is found to be very similar for the straight chain alkyl benzoates. The packing fraction at which the transition occurs for each of the compounds is shown in Figure 4. The lines in the figure show the packing fraction for each compound as a function of density. The open symbols indicate the packing fraction at ambient temperature and pressure, and the solid symbols indicate the transition points. For EB, PB, BB, and HB, the transition between the two regions is observed at about $\rho^* = 0.64$. For EHB, the only branched chain benzoate in this experiment, the transition packing fraction is higher, $\rho^* = 0.67$.

The rate of decrease in $\Delta\nu$ with increasing packing fraction, which is represented by the slope for the lines in the high-pressure region, is shown in Figure 5. The magnitude of the slope increases as the length of alkyl side chain increases. This indicates that for longer chain benzoates the effect of reducing the molar volume, or increasing the pressure, is greater than for the short chain alkyl benzoates.

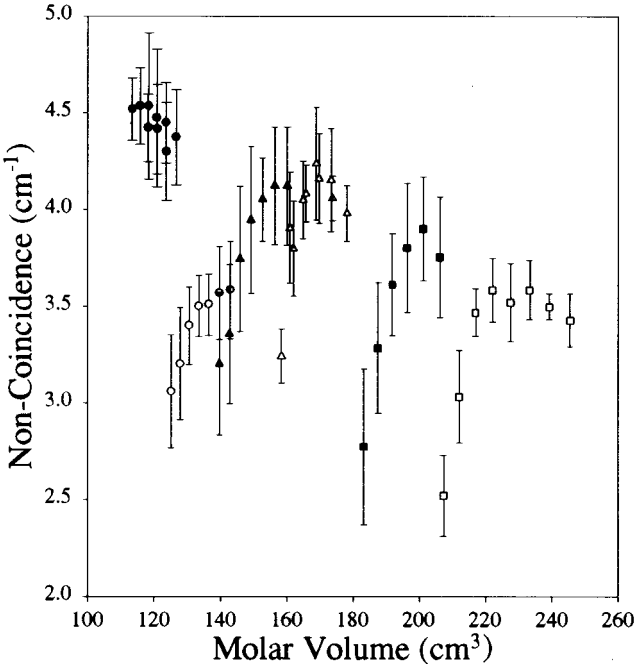

Figure 2. Noncoincidence values of the alkyl benzoates as a function of molar volume: MB (●), EB (○), PB (▲), BB (△), HB (■), and EHB (□). Error bars are calculated from the standard deviation of the repeated measurements.

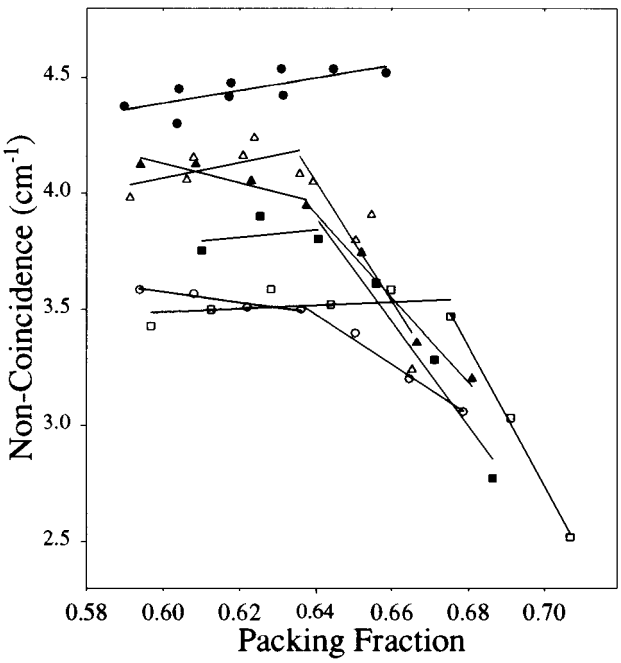

Figure 3. Noncoincidence values of the alkyl benzoates as a function of packing fraction: MB (●), EB (○), PB (▲), BB (△), HB (■), and EHB (□). Error in points is the same as the error shown in Figure 2.

Conformational Search and Molecular Mechanics Calculations. The conformation of alkyl benzoates investigated in the present study can be described by several torsional angles, as shown in Figure 6 for EHB. ϕ_0 was included for completeness, although it is commonly considered to be fixed at 0° due to the conjugation of phenyl ring and carbonyl group. Methyl rotation has been ignored in the conformational searches for

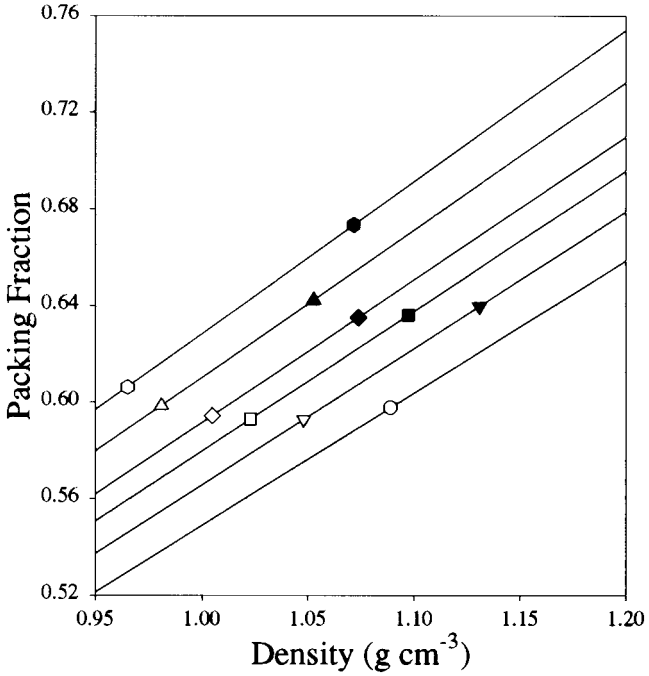

Figure 4. Transition packing fraction of the alkyl benzoates. A detailed explanation is given in the text. MB (○), EB (▽), PB (□), BB (◇), HB (△), and EHB (⬡).

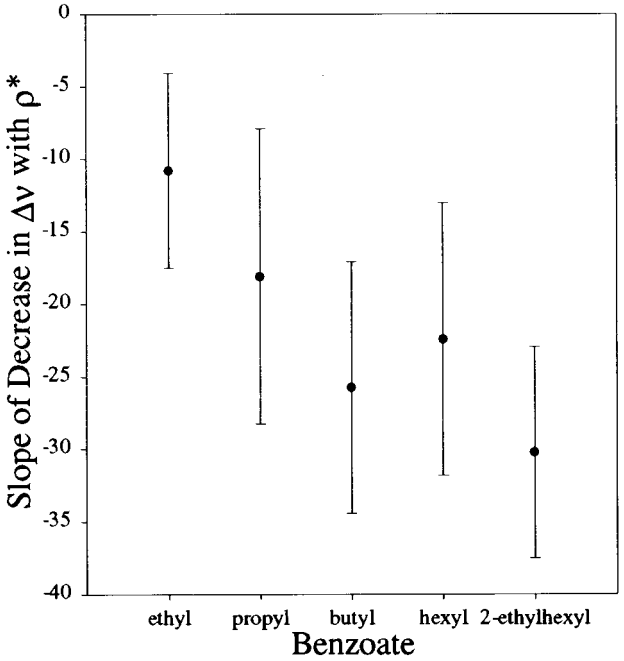

Figure 5. Slope of the decrease in noncoincidence with increasing packing fraction above the transition packing fraction vs chain length.

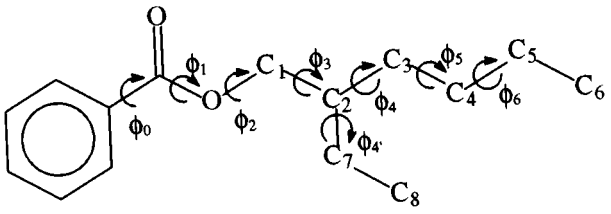

Figure 6. Torsional angles ($\phi_0-\phi_6$) and carbon atom numbering (C_1-C_8) used for the conformational study of a homologous series of unbranched alkyl benzoates and EHB.

the alkyl benzoates. For short chain alkyl benzoates, such as MB, EB, and PB, possessing relatively small numbers of torsional variables, the obvious generating method for starting

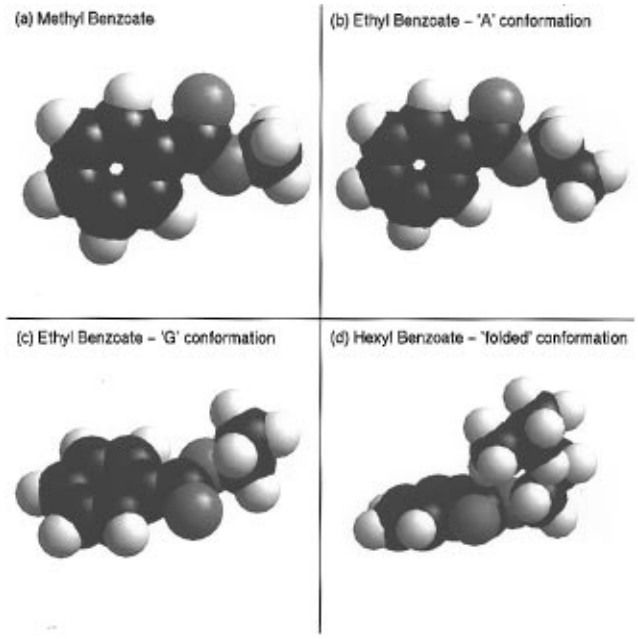

Figure 7. Energy-minimized conformations of (a) methyl benzoate, (b) A conformer of ethyl benzoate, (c) G conformer of ethyl benzoate, and (d) a folded conformer of hexyl benzoate.

geometry is a grid search with relatively high torsional angle resolution. The starting geometries for longer chain alkyl benzoates (C_n, $n \geq 4$, where n is the number of alkyl carbons) were generated from the conformers of C_{n-1} benzoate by replacing a hydrogen atom with a methyl group, and only from the energetically allowable conformers of C_{n-1} (within the threshold value). This strategy is based on two implicit assumptions. First, the torsional angles far away from carbonyl group (ϕ_4, ϕ_5, and ϕ_6) can have either anti or gauche conformations, as is seen for C−C bonds in *n*-alkanes. The second assumption is that replacing the hydrogen atom of the energetically unacceptable conformer of C_{n-1} (mostly due to close interatomic contacts) by the larger methyl group would also yield an energetically unacceptable conformer of C_n. With the initial geometries obtained by this manner, all the unique and stable conformers (or local minima) within 5 kcal/mol relative to the lowest energy conformation (global minimum) of each alkyl benzoate were obtained.

For MB only one stable conformation (global minimum) was found, in which all non-hydrogen atoms lie in the same plane ($\phi_0 = 0°/180°$, $\phi_1 = 180°$). The methyl group is in the trans (Z) conformation to the phenyl group, which is the case for the structure of most esters.[57] This structure also agrees with the results by semiempirical MO calculations.[58,59] The UFF energy minimized conformation of MB is shown in Figure 7a.

Three unique conformers of EB with different ϕ_2 were found within the energy threshold (5 kcal/mol). The strain energy profile for rotating the O−C_1 bond (ϕ_2) in EB is compared in Figure 8 with the well-known torsional energy profile for *n*-butane. The lowest energy conformation (the global minimum) for EB was found to be the planar zigzag structure with the terminal methyl group anti to the carbonyl group (A in Figure 8, $\phi_2 = 180°$). This structure is similar to the geometry obtained by another force field calculation[60] with slight differences in bond lengths and angles. A pair of local minima were also located with the terminal methyl group gauche to the carbonyl (G in Figure 8, $\phi_2 = \pm 74°$). The torsional angle ϕ_2 in the G conformers deviates from the normal gauche value ($\pm 60°$) due to the repulsion between the carbonyl oxygen and terminal methyl group. In addition to these expected local

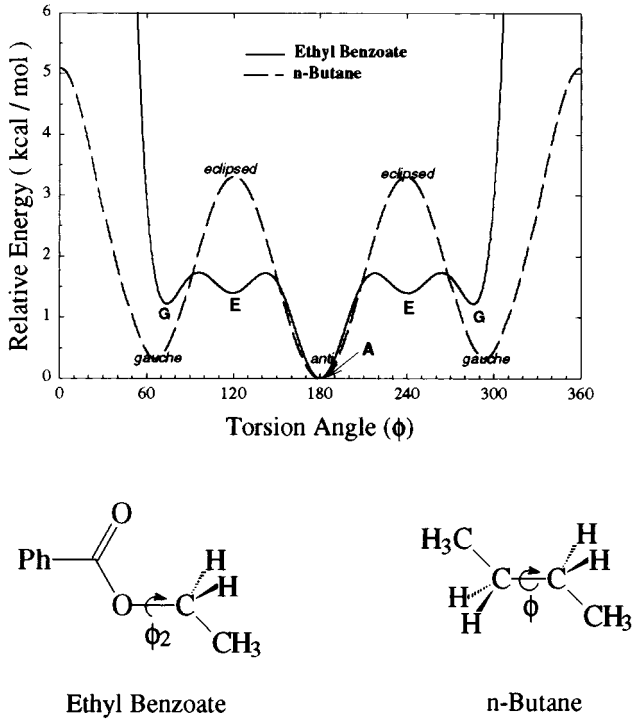

Figure 8. Torsional potential energy profile of ϕ_2 in ethyl benzoate compared with the energy profile of the central C−C bond in *n*-butane.

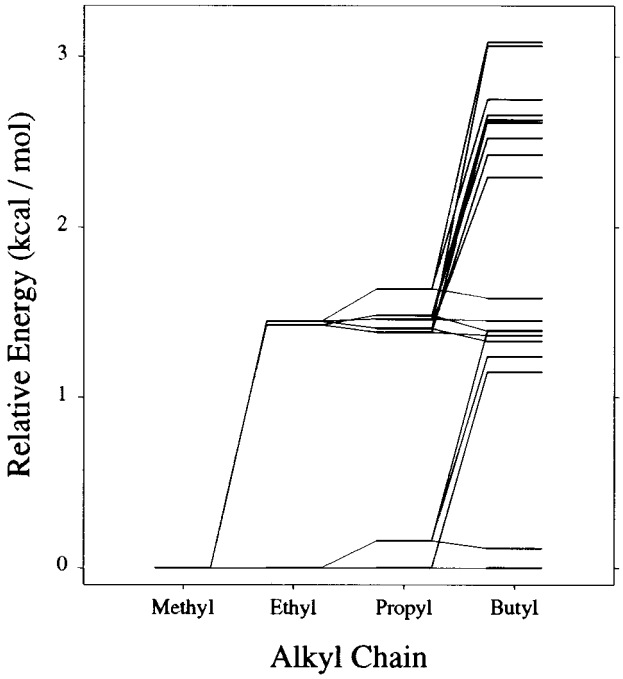

Figure 9. Diagram of relative energies of all local minimum conformations for methyl, ethyl, propyl, and butyl benzoates and the interrelationship between the conformers of each compound.

minima, another pair of local minima (E in Figure 8) were found with the eclipsed conformation ($\phi_2 = \pm 120°$). The energy barrier between these conformers (A ↔ E ↔ G) is relatively low, compared with that in *n*-butane (anti ↔ gauche). The existence of extra local minima (E) besides regular anti/gauche conformations shows the difference between C(═O)−O bond rotation and alkyl C−C rotation. The experimental results by microwave spectroscopy on the conformation of ethyl formate[61] were interpreted by the presence of two rotational isomers, one planar trans isomer (equivalent to A in EB) and one gauche isomer, slightly higher in energy, where the terminal methyl group is out of plane by 95° and is almost equal to the average ϕ_2 of G and E conformer in EB. Parts b and c of Figure 7 show the energy-minimized structure of the A and G conformers, respectively. The interactions between carbonyl groups are partially blocked by the terminal methyl group in the G conformation (also in E conformer not shown here).

For PB, seven unique conformers were found within the potential energy threshold. Among the seven conformers of PB, the conformer with fully extended, planar zigzag structure is the lowest energy conformation. All the energy-minimized PB conformers can be correlated with three EB conformers by adding ϕ_3 in anti or gauche conformations, although the G− conformation in ϕ_3 combined with G+ in ϕ_2 did not form a stable local minimum due to the repulsion between the carbonyl oxygen and methyl group. For BB, 20 unique conformers were found. For some of these conformers, especially with "folded" alkyl chain conformations, torsional angles (ϕ_3 and ϕ_4) deviate from regular anti/gauche values (180° or ±60°). In this way, possible close contact between methyl end and carbonyl group resulting in strong repulsion could be avoided by the relatively long *n*-butyl chain. Figure 9 is a graphical representation of the relative energies of all the local minimum for *n*-alkyl benzoates up to BB with the correlation between them. As shown in Figure 9, the energy differences between the various possible conformers are small.

All the anti or gauche conformations in ϕ_5 and ϕ_6 form low-energy local minima. As a result, 59 and 176 unique conformers were found for *n*-pentyl benzoate and HB, respectively. As in the BB case, the close atomic contact occurring in some conformers was effectively avoided in these relatively long alkyl side chains by slight modification of intermediate torsional angles from regular anti/gauche angles. One of the HB conformers with the "folded" alkyl side chain is shown in Figure 7d. Owing to the longer alkyl chain in HB, the surrounding of the carbonyl group of the conformer is more effectively shielded than in a conformer of EB shown in Figure 7c.

The conformational behavior of C-2 branched alkyl chain including EHB is almost the same as for the unbranched alkyl chains described above. An interesting point is that, with the gauche conformation in ϕ_2, only one conformation of ϕ_3 is allowed to form a low-energy local minimum. With two methylene groups attached to C-2 carbon, only one conformation out of three possible for ϕ_3 is allowed with the combination of the gauche conformation of ϕ_2 in order to avoid the repulsion with carbonyl oxygen.

Discussion

Although the conformational search in this study was performed without considering pressure and intermolecular interactions, the possible conformations and their relative energies are still useful because it is known that the application of external pressure of the range used in this experiment does not alter bond lengths or bond angles of the molecules. The only possible changes induced by this pressure range are the changes in intermolecular distances and the conformations of flexible alkyl chains. For all alkyl benzoates other than MB, the conformers with the "folded" side chain exist, and the energy difference between "folded" and "extended" conformations is only a few kcal/mol. This result is comparable with the molecular mechanics study[62] on the conformational preferences in alkylbenzenes and aryl−alkyl amines with a side chain of 3∼4 carbons long, where the energy of the folded conformation with the alkyl chain coiled toward the aromatic ring was calculated to be nearly the same or even lower than the energy of the extended conformer.

As mentioned in the Introduction, the increase in density generally results in the increase in $\Delta\nu$ due to the stronger interaction of two vibrational modes at smaller intermolecular distances. To the best of our knowledge, a decrease in the magnitude of noncoincidence with increasing density has been reported only for the C−O stretching band of methanol[21] and ethanol.[20] This was interpreted in terms of hydrogen bonding, which cannot contribute to the present case. We attribute the decrease in $\Delta\nu$ at higher pressure to a preference for the "folded" conformation under pressure, in which the alkyl chain is bent toward the aromatic ring and carbonyl group. According to the results of the conformational analysis, the fully extended conformation with the carbonyl group completely exposed to the neighboring molecules is the lowest energy conformation for unbranched alkyl benzoates. The relative population of this conformer is most likely to be high under atmospheric pressure. If the relative population of conformers with folded alkyl side chain increases, the average interaction between two carbonyl vibrational modes on neighboring molecules would be reduced due to the steric shielding of the carbonyl group by the folded alkyl chain. This would result in a decrease in $\Delta\nu$.

The question about the conformational preferences under higher pressure cannot be explicitly answered by the conformational study. Considering the fact that the relative molecular volume is the main factor affecting the relative population of the conformers, however, an increased population of the folded conformers at higher pressure should occur owing to the compact nature of the folded conformers. It is known that in hydrocarbon chains the volume of methylene unit is smaller in the gauche conformation than in the trans conformation.[39,44] Since the folded side chains in alkyl benzoates are formed by a series of gauche conformations, the volume of the folded conformers would be smaller than that of extended forms. A recent experiment on a homologous series of alkanes[63] has shown that alkanes have a tendency to fold to a quasispherical shape under pressure, which also supports this argument. Under high pressure, the slight energetic disadvantages of the folded conformer of the alkyl benzoates are largely overcome by the advantage in volume. As pressure increases beyond the transition point, the relative population of the folded form increases compared to the extended form, resulting in the continuous decrease in $\Delta\nu$. In the case of MB, only one conformer is possible. Therefore, $\Delta\nu$ is relatively insensitive to changes in pressure throughout the whole pressure range investigated. As the chain length increases, the alkyl chain can shield the carbonyl group more effectively as is shown for EB and HB in Figure 7c,d. This increasingly effective shielding in longer chains seems to be the main reason for the larger rate of decrease seen in $\Delta\nu$ in Figure 5.

The existence of the transition point can be explained in the following way. At the first stage of compression, the empty space (or free volume) in the liquid is decreased without much influence on the conformation of the molecules. As the empty space decreases, the intermolecular distances become smaller, and with further increase of pressure, the repulsive forces operating at smaller intermolecular distances compel the molecules to change conformation to the compact form. According to this interpretation, the point at which the noncoincidence starts to decrease corresponds to the density, or packing fraction, above which the intermolecular distances are so close that the interaction between molecules would induce the change of the conformation of the molecules. For all unbranched alkyl benzoates other than MB, the transition between the two regions was observed at about $\rho^* = 0.64$, as shown in Figure 4. It is interesting to note that 0.64 is the packing fraction of random close-packed spheres,[64−66] which is the most compact packing possible for spheres without introducing crystalline order. For EHB, with a branched alkyl chain, the transition is at a higher packing fraction, which may be due to either a less spherical folded conformation[56] or a smaller volume change upon folding, reducing the preference for the folded conformer.

Acknowledgment. This material is based on work supported under a National Science Foundation Graduate Research Fellowship and in part by the NSF under Grant CHE 95-26237 and by the Air Force Office for Science Research under Grant AFOSR F49620-93-1-0241.

References and Notes

(1) Schindler, W.; Sharko, P. T.; Jonas, J. *J. Chem. Phys.* **1982**, *76*, 3493−3496.
(2) Bradley, M. S.; Krech, J. H. *J. Phys. Chem.* **1993**, *97*, 575−580.
(3) Torii, H. *J. Mol. Struct. (THEOCHEM)* **1994**, *311*, 199−203.
(4) Thomas, H. D.; Jonas, J. *J. Chem. Phys.* **1989**, *90*, 4144−4149.
(5) Shelley, V. M.; Yarwood, J. *Mol. Phys.* **1991**, *72*, 1407−1423.
(6) Shelley, V. M.; Yarwood, J. *Chem. Phys.* **1989**, *137*, 277−280.
(7) Sun, T. F.; Chan, J. B.; Wallen, S. L.; Jonas, J. *J. Chem. Phys.* **1991**, *94*, 7486−7493.
(8) Schindler, W.; Zerda, T. W.; Jonas, J. *J. Chem. Phys.* **1984**, *81*, 4306−4313.
(9) Purkayastha, A.; Kumar, K. *Spectrochim. Acta* **1987**, *43A*, 1269−1274.
(10) Scheibe, D. *J. Raman Spectrosc.* **1982**, *13*, 103−109.
(11) Wang, C. H.; McHale, J. *J. Chem. Phys.* **1980**, *72*, 4039−4044.
(12) McHale, J. *J. Chem. Phys.* **1981**, *75*, 30−35.
(13) McHale, J. *J. Chem. Phys.* **1982**, *77*, 2705−2707.
(14) Mirone, P.; Fini, G. *J. Chem. Phys.* **1979**, *71*, 2241−2243.
(15) Giorgini, M. G.; Fini, G.; Mirone, P. *J. Chem. Phys.* **1983**, *79*, 639−643.
(16) Logan, D. E. *Mol. Phys.* **1986**, *58*, 97−129.
(17) Logan, D. E. *Chem. Phys.* **1986**, *103*, 215−225.
(18) Logan, D. E. *Chem. Phys.* **1989**, *131*, 199−207.
(19) Mirone, P.; Fini, G. *J. Chem. Soc., Faraday Trans. 2* **1974**, *70*, 1776−1782.
(20) Thomas, H. D.; Jonas, J. *J. Chem. Phys.* **1989**, *90*, 4632−4633.
(21) Zerda, T. W.; Thomas, H. D.; Bradley, M.; Jonas, J. *J. Chem. Phys.* **1987**, *86*, 3219−3224.
(22) Adamy, S. T.; Grandinetti, P. J.; Masuda, Y.; Campbell, D. M.; Jonas, J. *J. Chem. Phys.* **1991**, *94*, 3568−3575.
(23) Jonas, J.; Adamy, S. T.; Grandinetti, P. J.; Masuda, Y.; Morris, S. J.; Campbell, D. M.; Li, Y. *J. Phys. Chem.* **1990**, *94*, 1157−1164.
(24) Walker, N. A.; Lamb, D. M.; Adamy, S. T.; Jonas, J.; Dare-Edwards, M. P. *J. Phys. Chem.* **1988**, *92*, 3675−3679.
(25) Zhang, J.; Jonas, J. *J. Phys. Chem.* **1994**, *98*, 6835−6839.
(26) Adamy, S. T.; Kerrick, S. T.; Jonas, J. *Z. Phys. Chem. (Munich)* **1994**, *184*, 185−203.
(27) Whitley, A.; Yarwood, J.; Gardiner, D. J. *J. Chem. Soc., Faraday Trans.* **1993**, *89*, 881−884.
(28) Whitley, A.; Yarwood, J.; Gardiner, D. J. *J. Mol. Struct. (THEOCHEM)* **1991**, *247*, 187
(29) Whitley, A.; Yarwood, J.; Gardiner, D. J. *Ber. Bunsen-Ges. Phys. Chem.* **1990**, *94*, 404−407.
(30) Slager, V. L.; Chang, H.-C.; Jonas, J. *J. Raman Spectrosc.* **1996**, *27*, 799−803.
(31) Jonas, J. *J. Chem. Soc., Faraday Trans. 2* **1987**, *83*, 1777−1789.
(32) Schindler, W.; Jonas, J. *J. Chem. Phys.* **1980**, *72*, 5019−5025.
(33) Schroeder, J.; Schiemann, V. H.; Sharko, P. T.; Jonas, J. *J. Chem. Phys.* **1977**, *66*, 3215−3226.
(34) Campbell, J. H.; Fisher, J. F.; Jonas, J. *J. Chem. Phys.* **1974**, *61*, 346−360.
(35) Schroeder, J.; Schiemann, V. H.; Jonas, J. *J. Chem. Phys.* **1978**, *69*, 5479−5488.
(36) Isaacs, N. S. *Liquid-Phase High-Pressure Chemistry*; John Wiley & Sons, Inc.: Chichester, 1981.
(37) Ando, I.; Webb, G. *Magn. Reson. Chem.* **1986**, *24*, 557−567.
(38) Schoen, P. E.; Priest, R. G.; Sheridan, J. P.; Schnur, J. M. *Nature* **1977**, *270*, 412−414.
(39) Wong, P. T. T.; Mantsch, H. H.; Snyder, R. G. *J. Chem. Phys.* **1983**, *79*, 2369−2374.
(40) Bassett, D. C. *Principles of Polymer Morphology*; Cambridge University Press: New York, 1981.
(41) Bonev, B. B.; Morrow, M. R. *Biophys. J.* **1995**, *69*, 518−523.

(42) Wong, P. T. T.; Mantsch, H. H. *J. Chem. Phys.* **1985**, *83*, 3268−3274.
(43) Ando, I.; Inoue, Y. *Makromol. Chem., Rapid Commun.* **1983**, *4*, 753−757.
(44) Wong, P. T. T.; Chagwedera, T. E.; Mantsch, H. H. *J. Chem. Phys.* **1987**, *87*, 4487−4497.
(45) Snyder, R. G. *J. Chem. Phys.* **1982**, *76*, 3342−3343.
(46) Leach, A. R. In *Reviews in Computational Chemistry*; Lipkowitz, K. B., Boyd, D. B., Eds.; VCH Publishers: New York, 1991; Vol. 2.
(47) Saunders, M.; Houk, K. N.; Wu, Y.-D.; Still, W. C.; Lipton, M.; Chang, G.; Guida, W. C. *J. Am. Chem. Soc.* **1990**, *112*, 1419−1427.
(48) Kolossváry, I.; Guida, W. C. *J. Am. Chem. Soc.* **1996**, *118*, 5011−5019 and references therein.
(49) Lipton, M.; Still, W. C. *J. Comput. Chem.* **1988**, *9*, 343−355.
(50) Akai, J. A. Ph.D. Thesis, University of Illinois, 1977.
(51) Jonas, J.; Hasha, D.; Huang, S. G. *J. Chem. Phys.* **1979**, *71*, 3996−4000.
(52) Wallen, S. L.; Nikiel, L.; Yi, J.; Jonas, J. *J. Phys. Chem.* **1995**, *99*, 15421−15427.
(53) Rappé, A. K.; Casewit, C. J.; Colwell, K. S.; Goddard, W. A., III; Skiff, W. M. *J. Am. Chem. Soc.* **1992**, *114*, 10024−10035.
(54) Casewit, C. J.; Colwell, K. S.; Rappé, A. K. *J. Am. Chem. Soc.* **1992**, *114*, 10035−10046.
(55) Fletcher, R.; Reeves, C. M. *Comput. J.* **1964**, *7*, 149−154.
(56) Bondi, A. *Physical Properties of Molecular Crystals, Liquids, and Glasses*; John Wiley & Sons, Inc.: New York, 1968.
(57) Eliel, E. L.; Wilen, S. H.; Mander, L. N *Stereochemistry of Organic Compounds*; Wiley & Sons, Inc.: New York, 1994.
(58) Diehl, P.; Huber, H.; Kunwar, A. C.; Reinhold: M. *Org. Magn. Reson.* **1977**, *9*, 374−378.
(59) Mendicuti, F.; Saiz, E.; Patel, B.; Dodge, R.; Mattice, W. L. *J. Phys. Chem.* **1990**, *94*, 8374−8378.
(60) Ystenes, M.; Rytter, E. *Spectrochim. Acta* **1989**, *45A*, 1127−1135.
(61) Riveros, J. M.; Wilson, Jr., E. B. *J. Chem. Phys.* **1967**, *46*, 4605−4612.
(62) Grunewald, G. L.; Creese, M. W.; Weintraub, H. J. R. *J. Comput. Chem.* **1988**, *9*, 315−326.
(63) Brüsewitz, M.; Weiss, A. *Ber. Bunsen-Ges. Phys. Chem.* **1993**, *97*, 1−9.
(64) Bernal, J. D.; Mason, J. *Nature* **1960**, *188*, 910−911.
(65) Scott, G. D. *Nature* **1960**, *188*, 908−909.
(66) Berryman, J. G. *Phys. Rev. A* **1983**, *27*, 1053−1061.